5.2 NONHYDROSTATIC SIMULATIONS OF OROGRAPHIC FLOWS AND SOME EFFECTS OF TIME INTEGRATION SCHEMES

Raffaele Salerno
Epson Meteo Center (Centro Epson Meteo, CEM), Cinisello Balsamo (MI), Italy

1.INTRODUCTION

In the past, but still at the present time, weather prediction models have extensively used hydrostatic approximation, in order to avoid acoustic waves in the vertical direction. Usually, nonhydrostatic (NHY) effects may be negligible for scales larger than 100 km and the hydrostatic (HY) assumption is a good approximation that is well respected in the atmosphere down to scales of 10-15 km. However, the dynamical effects excluded by the HY assumption, for example the propagating wave breaking and overturning, start to become non-negligible and the use of NHY models is necessary. One consequence of NHY modelling is the necessity to solve a full 3D Poisson or Helmoltz equation, but some minor overhead due to this is adequately balanced by the capture of a broad range of flows even at the planetary scale (Smolarkiewicz et al., 2001).

NHY models can be divided into two categories: those containing fast acoustic modes (compressible) and those that filter such modes by certain types of approximation (anelastic). Examples of the former are, among others, MC2 (Benoit et al., 1997), MRI/JMA-NHM (Saito et al., 2001) and WRF (www.wrf-model.org), while, for the latter, an example is the Meso-NH model (Bougeault and Mascart, 2001). In the anelastic case, the vertical acoustic modes are treated implicitly to remove the time step limitation due to the Courant-Frederich-Levy (CFL) stability condition.

With high-frequency acoustic waves, a very small time step is required to prevent numerical instabilities in an explicit time scheme. In the recent times, fully compressible NHY models have become more popular, following the improvement of numerical techniques and computational resources. Better time schemes, like explicit time-splitting, have been introduced in NHY models (Klemp and Williamson, 1978), reducing computational times; but the implementation of the semi-implicit technique has been a considerable development in numerical atmospheric models, relaxing the strict constraint of extremely small time steps (e.g. Tapp and White, 1976; Juang, 1992), due to its capability to slow down the fastest propagating waves.

In the alpine area and peninsular Italy, it is very important to consider grid resolutions as well as a detailed description of vertical motions. In this region, the atmospheric behaviour might depend strongly on NHY processes, such as mountain waves, penetrative convection and orographically-enhanced storms.

Depending on stability conditions (Pielke, 1984), with fine horizontal grid mesh sizes it is not possible to retain HY approximations. In particular, if a model has to be applied in a typical mesoscale domain, it should use the NHY primitive equations. In a few models, an hydrostatic-pressure vertical coordinate can be used permitting a switch-controlled choice between the HY primitive equations (for large-and synoptic-scale applications), and the NHY primitive equations (for smaller-scale applications).

Orography strongly affects the motion across a long ridge of mountains and, when waves in the x-z vertical plane develop, several weather phenomena, that significantly affect human activities, are produced. As an example, the strong downslope winds (Klemp and Lilly, 1975; Colle and Mass, 1998), observed along the lee slopes of mountain barriers are usually related to large-amplitude waves.

Fine resolutions, required in a very complex topography environment, may require high-order finite difference schemes and small time steps. Nevertheless, the required high-order accuracy is also achieved with spectral methods. They assure many advantages, including the absence of the truncation error in linear terms, the absence of aliasing and phase errors and an efficient use of semi-implicit time integration. In this work, test runs made by CEM multiscale spectral model, in the nonhydrostatic, semi-implicit and semi-Lagrangian versions, have been performed. Particularly, results using different grid resolutions (20, 10, 5 and 3 km) for variable domains (fig. 1) have been analysed for some real cases, comparing simulations made in different configurations, characterized by the steep orographic gradients of alpine regions. Differences among HY and NHY simulations at different resolutions in a complex topography have been analyzed in a previous work, comparing many runs made with different horizontal mesh sizes (Salerno and Borroni, 2002), where the model domains used coarser grids respect to this work, even if they covered the same areas. Cascade runs have been performed in the

* *Corresponding author address*: Raffaele Salerno, Centro Epson Meteo, Research and Development Division, via de Vizzi 93/95, 20090 Cinisello Balsamo (MI), Italy; e-mail: raffaele.salerno@epson-meteo.org

current one-way nesting environment; the characteristics of the finest grid domain have been firstly chosen, according to the phenomenon being examined. After that, the sequence of coarser runs has been established.

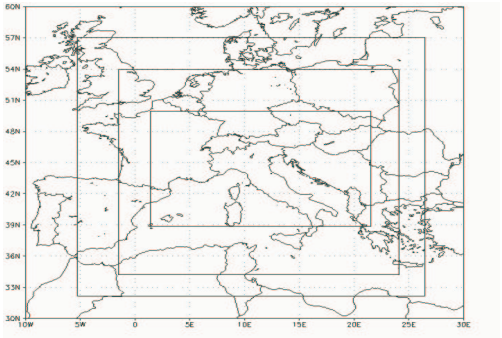

Figure 1. Integration domains for real case studies. The full large area is for 20 km grid mesh size, the smallest for 3 km grid.

Multiple simulations have also been made for idealized mountains, analysing also flow regimes at various Froude numbers. The differences between simulations, made by using the semi-implicit, semi-lagrangian time scheme or the semi-implicit one only, have been explored, also using some idealized tests at various CFL numbers. A few results are presented here to show the basic characteristics of the different simulations and conditions.

Due to the meteorological help given to a team involved with flight records by a motor sailplane in South America, daily simulations of orographic flows have been performed around the mountain regions of this area from November 2003 to January 2004. So, results have been analyzed for the Andes central and southern region. A comparison, among the computations in different configurations, has been made and a few results will be also shown.

2.MODEL DESCRIPTION

A brief summary of the NHY formulation of the model will be given. An hydrostatic-pressure vertical coordinate is used for HY and NHY primitive equations. The fully-compressible NHY system can be written as:

$$\frac{dU}{dt} = fV - K\frac{\partial S}{\partial x} - RT\frac{\partial q}{\partial x} - \frac{T}{\overline{T}}\frac{\partial q}{\partial(\ln\sigma)}\frac{\partial\overline{\Phi}}{\partial x} + F_U$$

$$\frac{dV}{dt} = -fU - K\frac{\partial S}{\partial y} - RT\frac{\partial q}{\partial y} - \frac{T}{\overline{T}}\frac{\partial q}{\partial(\ln\sigma)}\frac{\partial\overline{\Phi}}{\partial y} + F_V$$

$$\delta\frac{dW}{dt} = -g + g\frac{T}{\overline{T}}\frac{\partial q}{\partial(\ln\sigma)} + F_W$$

$$\frac{C_v}{C_p}\frac{dq}{dt} = -S\left(\frac{\partial U}{\partial X} + \frac{\partial V}{\partial y} + \frac{\sigma}{R\overline{T}}\frac{\partial U}{\partial\sigma}\frac{\partial\overline{\Phi}}{\partial x} + \frac{\sigma}{R\overline{T}}\frac{\partial V}{\partial\sigma}\frac{\partial\overline{\Phi}}{\partial y}\right) + \frac{g\sigma}{R\overline{T}}\frac{\partial w}{\partial\sigma} + \frac{F_T}{T}$$

$$\frac{dT}{dt} = \frac{R}{C_p}T\frac{dq}{dt} + F_T$$

$$\frac{dQ}{dt} = F_Q$$

where q = ln(p), δ is one for NHY runs and zero for the HY ones, S is the square of the map scale factor, *m*, and K is

$$K = \frac{1}{2}\left(U^2 + V^2\right).$$

The total derivative

$$\frac{d}{dt} = \frac{\partial}{\partial t} + S\left(U\frac{\partial}{\partial x} + V\frac{\partial}{\partial y}\right) + \dot{\sigma}\frac{\partial}{\partial\sigma}$$

is expressed in terms of the horizontal wind images,

$$\begin{pmatrix} U \\ V \end{pmatrix} = \frac{1}{m}\begin{pmatrix} -\sin\lambda & -\cos\lambda \\ \cos\lambda & -\sin\lambda \end{pmatrix}\begin{pmatrix} u \\ v \end{pmatrix}$$

Conservation of total energy is assured if the continuity equation is strictly retained. The time integration is both semi-implicit and semi-implicit semi-Lagrangian. Lateral boundary relaxation is considered; it may be either explicit or implicit, time-splitting. A lateral boundary blending may be also considered and 4th order horizontal diffusion is applied. Perturbation method is applied for the resolution of the equation in the model, because zero lateral boundary condition can be satisfied and diffusion can be applied to perturbation only (Juang, 1992), since non-zero boundary conditions may cause serious difficulties with semi-implicit time schemes. The model uses a type of dynamical initialization which can be considered whenever there is a doubt about the balance state of the initial conditions or when a field such as vertical motion is not given in the initial analysis. But the inizialization on the finer meshes is omitted when these are driven by coarser runs. Flux computation in the surface layer follows the Monin-Obukhov similarity profile (Arya, 1988) with a multi-layer soil model in which different classes of vegetation and soil types are considered. Vertical turbulent eddy diffusion of momentum, heat and vapour is computed in this study via a non-local approach in the boundary layer where in the free atmosphere the formulation is based on scale parameters obtained from observation. Deep convection has been treated with a relaxed Arakawa-Schubert scheme (Moorthi and Suarez, 1992-1999; a modified Grell scheme and Kain-Fritsch (1993) parameterization are available). The microphysics treatment employs five prognostic species including water vapour, cloud water, cloud ice, snow and rain (Rutledge and Hobbs, 1989).

3.IDEALIZED TEST RUNS

Many test runs have been made in both HY incompressible and NHY compressible mode. The sensitivity of the model to the range of flows in idealized non-linear two-dimensional analysis was tested using an isolated mountain 800 m high and a reference horizontal wind of 10 m/s, investigating inverse Froude number flows ranging from 0.2 to 2 (Salerno and Borroni, 2002; Salerno, 2003). For this isolated mountain, an example of the pressure, horizontal and vertical velocity perturbations are shown in fig. 2.

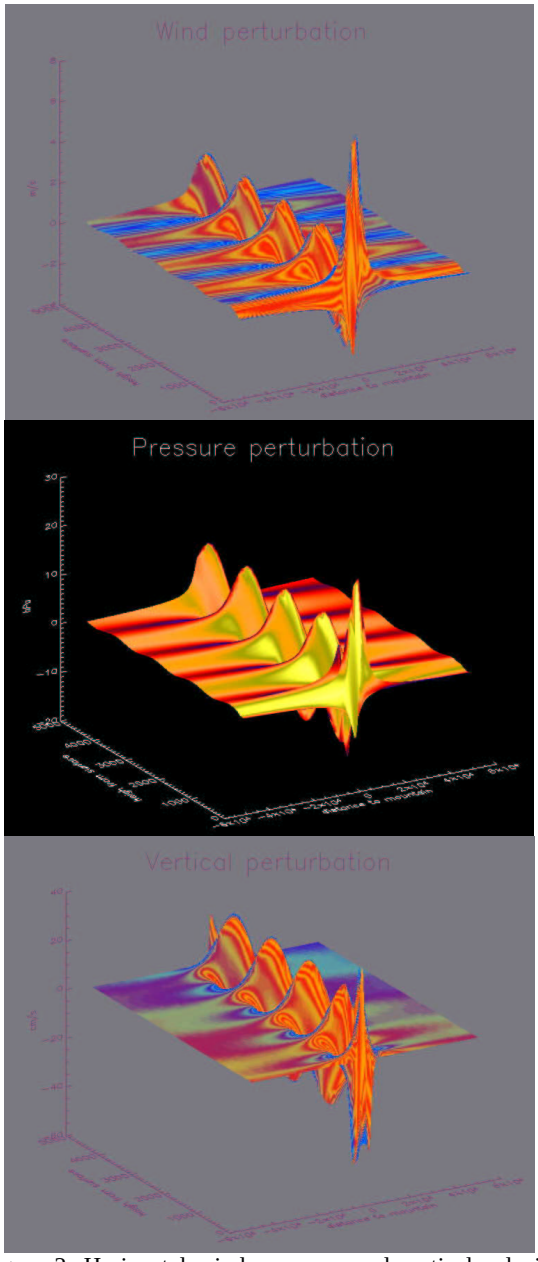

Figure 2. Horizontal wind, pressure and vertical velocity perturbation for an isolated, bell-shaped, 800 m height mountain.

About the SI-SL time-integration scheme, it is known that two kinds of resonance can occur when stationary forcings are introduced. The first kind is a quasi-barotropic resonance, which can occur both in shallow-water SI-SL systems as well as in 3D systems. The second kind is a very-short vertical-scale resonance, which can occur only in 3D systems. This is connected to the flow regimes. In an idealized context, the flow is hydrostatic when

$$\frac{2U}{LN} << \left(\frac{RT_*}{g}\right)^{0.5} H$$

where U is the flow speed, L is the mountain width, H is the height, N^2 is the Brünt-Väisälä frequency, T_* is the temperature at the reference state.

The hydrostatic hypothesis modifies the wave propagation, in a manner independent of the characteristic of the flow. This means that the geometrical characteristics of the flow can make the propagation nonhydrostatic even if the vertical velocities remain in the hydrostatic domain themselves.

There are some problems using the semi-implicit technique: gravity waves are excessively slowed down if a too large time-step is used. This may have consequences for the interactions of important dynamical processes and, therefore, this may lead to a less accurate representation of the cascade of energy. In the semi-lagrangian framework, as the equations are time-stepped along the advective characteristic lines, there are no limitations imposed by numerical stability on the magnitude of the time-step due to the advective terms. Therefore, the method is effective only if there is not too much energy at the smallest scales. In the SI-SL version, there is no limitations due to stability regarding time-step magnitude with respect to any physical process described by the momentum equations. However, the presence of orography may be troublesome in semi-Lagrangian methods, effectively reducing the allowable time-step. SI-SL is also related to the same problems as in the semi-implicit methods alone.

To ideally reproduce a north-south mountain chain as in South America, simulations have been performed for an elongated mountain (i.e. with x << y) of 3000 m of height and homogeneous in the direction perpendicular to an upcoming stratified flow.

The vertical wavenumber scale of the internal gravity waves is of the order of N/U. When the horizontal length-scale is longer than the vertical, the horizontal component of the group velocity has the magnitude of U. Waves with vertical wavenumber less than N/U are able to propagate across, having a larger group velocity, and in the central part of the mountain the flow reproduces the two-dimensional case at the beginning, reaching a three-dimensional

form in a time with magnitude y/U. In the simulation, a length of 100 km along y has been chosen (and a zonal width of 10 km), then with a x-velocity of 10 m/s, this time is slightly less than three hours. In fig. 3, the Scorer parameter profile is represented for this simulation, after 12 h, in the centre of the mountain, upwind side, made in the condition which the Froude number is 2.

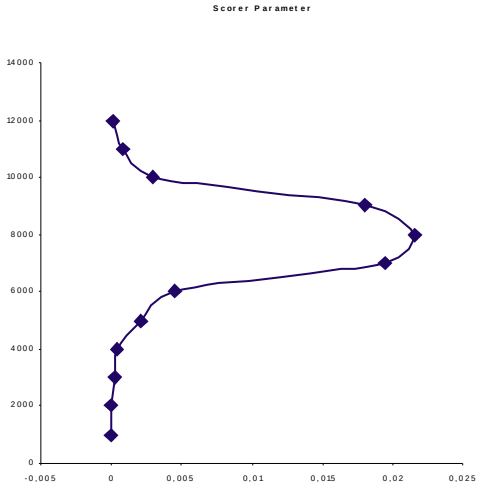

Figure 3. The Scorer parameter after 12 h of the idealized simulation at the centre of a 10 km width elongated mountain.

4.REAL CASE STUDIES

Results have been obtained from real situations analysed by the model over the domains depicted in fig. 1. Only a brief discussion on two real cases is presented here; other cases have been discussed in previous works (e.g. Salerno, 2003). Generally speaking, the propagation of mountain waves in some alpine areas is partially limited when a well-developed mixing occurs. Better identification of valley phenomena is, of course, achieved with increasing resolution. Only at 10 km of resolution or less, there is a better defined structure of vertical plumes in the NHY, due to well organized vertical motions. The circulation has more coherent structures, mainly due to the gaining of buoyancy in the generated propagating gravity waves. Also, more realistic less-pronounced upward velocities in the NHY simulations occur (than in the HY ones), respect to the stratification of the atmosphere in the lower layers. For precipitation, large grid simulations capture the location of the primary precipitation region but underestimate the magnitude of maxima as well as the total precipitation.

Another case regarding the southern Andes regions is also discussed here. This case study presents many flow regimes, and it may be a good depiction of orographic flows.

4.1 February, 23-24th, 2002

This case has been also discussed in previous works (e.g. Salerno, 2003). The case study has been revisited in the new experimental design with the grid mesh sizes of 20, 10, 5 and 3 km. Moreover, the topography database has been changed, and topography has been recomputed starting from a 90 m digital elevation model.

This situation was characterised by a large and deep low pressure area, placed between Iceland and Scandinavia, which drove cold air toward the alpine region. A cold front went across the Alps during the night between day 23 and 24 leading to föhn conditions in south alpine regions and staü in the northern parts. In the previous work, both HY and NHY runs showed a generally correct representation of föhn in southern Alps. Also, both 20 km and 10 km runs showed the same characteristics. In the new NHY simulations, structures are even better defined, and the importance of NHY effects have an evidence in all grid simulations, depending on the balance between buoyancy and gravity, and the angle between the winds and the mountains. With 5 and 3 km grid mesh size, the vertical structures in the NHY run are well organized.

Addressing the influence of time integration schemes on simulations, some problems arose with excessive time steps, and a slow-down of gravity waves occurred. The presence of energy at the smallest scale is more evident at the highest resolutions, leading to an energy transfer to longer wavelenghts.

4.2 October 6-7th, 2003

In this case, cold air was driven to the alpine region and, during the night between the 6th and 7th, it crossed the Alps, bringing föhn winds in sub-alpine regions of Piedmont and Lombardia, strong northwest winds all over Italy, an abrupt change of temperatures and heavy precipitations in central and southern Italy.

Simulations have been performed with the same experimental design. The results mainly confirmed the ones obtained in other simulations. For example, with a 10 km grid mesh size, the NHY characteristics are evident in the plume tilting and the wave structures (figs. 4 and 5)

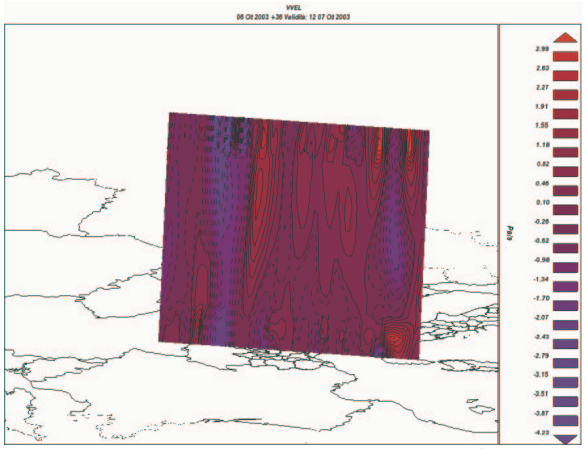

Figure 4. Longitudinal sections (at about 9° E) for vertical velocity with 10 km grid mesh size. Upward velocities are in the blue range.

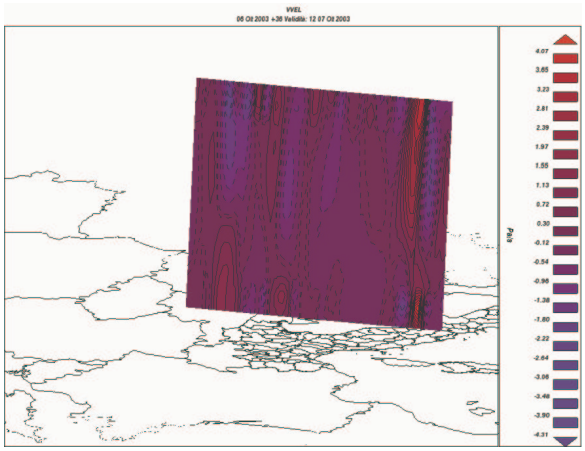

Figure 5. As in figure 4, at 12° E.

4.3November 24-25th, 2003, South America

A cold front was in the south of Chile up to a latitude of about 51 S. A WSW flux impacted on the north-south mountain chain issuing different flow regimes in the area between 49 S and 32 S. Particularly, high resolution simulations have been performed over an area between 40 S and 52 S. In this case, different flow regimes are fairly well evidenced depending on the surface characteristics. Around 41 S, mountain waves resembles the ones obtained in a quasi-uniform flow regime, as it can be seen in fig. 6. Around 44 S, waves show an abrupt change; lee waves are formed, as represented in fig. 7 but also confirmed by the photo taken in the same area (fig. 9). West of the mountain, the mountain waves are mixed to the flow due to the convection on the argentine Pampas. South of 51 S, the model topography is less steep and only weak waves are still present, depending on resolution. Indeed, the frontal structure is clearly evident (fig. 8).

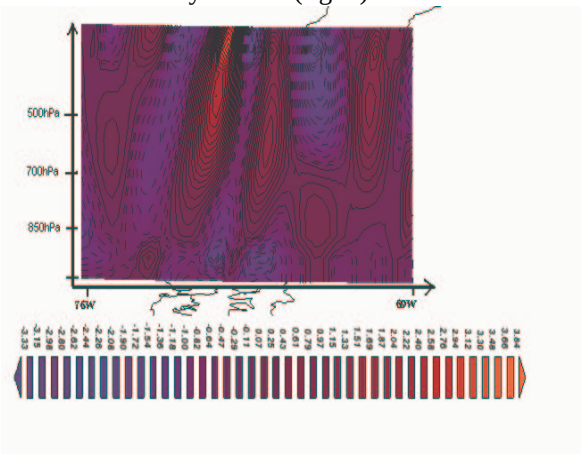

Figure 6. Section of vertical velocities at 41 S. This comes from the 10 km simulation. Upward velocities are in the blue range.

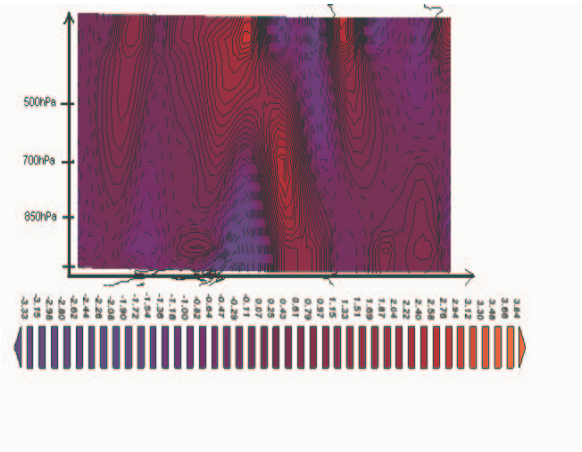

Figure 7. As in fig. 6 but at 44 S.

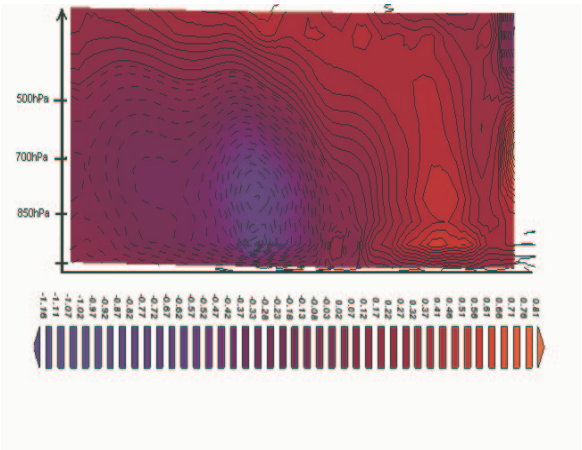

Figure 8. Same as fig. 6 but at 51° 30’ S.

Figure 9. A photo taken on November 25th, 2003 in the area at 44.2S and 70.25W, towards mountains, showing the lenticular clouds associated to the lee waves.

6.CONCLUSION

In the last decade, the growth of computer systems and the improvement of atmospheric physics algorithms have lead to a wider use of NHY models. The influence of vertical accelerations are important in topographically complex domains. Many runs, both test idealized and real cases, have been made by CEM multiscale model in NHY mode. Different resolution grids, centered in the Alps region, have been used for case studies as well as the central and southern Andes and Patagonia regions.

Test runs were made in ideal cases with isolated mountain of different heights and width and in a 2D and 3D configurations. An idealized case of an elongated but isolated mountain has been also performed. For this simulation, the vertical wavenumber scale of the propagating gravity waves is of the order of N/U. When the horizontal length-scale is longer than the vertical, the horizontal component of the group velocity has the magnitude of U. Waves with vertical wavenumber less than N/U are able to propagate across, having a larger group velocity, and in the central part of the mountain the flow reproduces the two-dimensional case at the beginning, reaching a three-dimensional form in a time with magnitude y/U.

About the SI-SL time-integration scheme, it is known that two kinds of resonance can occur when stationary forcings are introduced. The first kind is a quasi-barotropic resonance, which can occur both in shallow-water SI-SL systems as well as in 3D systems. The second kind is a very-short vertical-scale resonance, which can occur only in 3D systems and it is connected to the flow regimes.

There are some troubles using the semi-implicit technique: gravity waves are excessively slowed down if a too large time-step is used. This may have consequences for the interactions of important dynamical processes and, therefore, this may lead to a less accurate representation of the cascade of energy. The presence of orography is somewhat troublesome in the semi-Lagrangian context, effectively reducing the allowable time-step. SI-SL is also related to the same problems as in semi-implicit methods alone. Differences have been evidenced depending on the horizontal resolution.

Many real cases of mountain waves have been considered, only few results have been shown. In the simulations, structures are fairly well defined, and the importance of NHY effects have an evidence in all grid simulations, depending on the balance between buoyancy and gravity, and the angle between the winds and the mountains. With the finer grids of 5 and 3 km, the vertical structures are well organized evidencing the flow regimes. Vertical structures of propagating plumes of vertical motion were stronger and fairly well organized in the NHY mode runs.

References:

Arya, S. P., 1988 : Introduction to Micrometeorology. International Geophysics Series, vol. 42, Academic Press inc.

Benoit, R., M. Desgagne, P. Pellerin, Y. Chartier and S. Desjardins, 1997 : The canadian MC2 : a semi-lagrangian, semi-implicit wide-band atmospheric model suited for fine-scale process studies and simulation. Mon. Wea. Rev., **125**, 2382-2415.

Bougealt, P. and P. Mascart, 2001: The Meso-NH atmospheric simulation system: scientific documentation. MeteoFrance-CNRS Tech. Rep.

Colle, B.A., and C.F. Mass, 1998: Windstorms along the Western Side of the Washington Cascades. Part I: A High Resolution Observational and Modeling Study of the 12 February 1995 Event. Mon. Wea. Rev., **126**, 28-52.

Colle, B.A., and C.F. Mass, 1998: Windstorms along the Western Side of the Washington Cascades. Part II: Characteristics of Past Events and Three-Dimensional Idealized Simulations. Mon. Wea. Rev., **126**, 53-71.

Juang, H.-M. H., 1992: A Spectral Fully Compressible Nonhydrostatic Mesoscale Model in Hydrostatic Sigma Coordinates: Formulation and Preliminary Results. Meteor. Atmos. Phys., **50**, 75-88.

Kain, J. S., and J. M. Fritsch, 1993: Convective parameterization for mesoscale models: The Kain-Fritsch scheme. The representation of cumulus convection in numerical models. K. A. Emanuel and D. A. Raymond, Eds., Amer. Met. Soc., 246 pp.

Klemp, J.B., and D.K. Lilly, 1975: The Dynamics of Wave Induced Downslope Windstorms. J. Atmos. Sci., **32**, 320-339.

Klemp, J. B., and R. B. Wilhelmson, 1978: The Simulation of Three-Dimensional Convective Storm Dynamics. J. Atmos. Sci., **35**, 1070-1096.

Moorthi, S., and M.J. Suarez, 1992: Relaxed Arakawa-Schubert: A parameterization of moist convection for

general circulation models. Mon. Wea. Rev., **120**, 978-1002.

Moorthi, S., and M.J. Suarez, 1999: Documentation of version 2 of Relaxed Arakawa-Schubert cumulus parameterization with moist downdrafts. NOAA Technical report NWS/NCEP 99-01. 44pp.

Pielke, R.A., 1984: Mesoscale Meteorological Modeling. Academic Press, N.Y, 612 pp.

Rutledge, S. A. and P. V. Hobbs, 1983 : The mesoscale and microscale structure and organization of clouds and precipitation in midlatitude cyclones. Part VIII: A model for the "seeder-feeder" process in warm-frontal rainbands. *J. Atmos. Sci.*, **40**, 1185-1206.

Saito, K., T. Kato, H. Eito and C. Muroi, 2001: Documentation of the Meteorological Research Institute-Numerical Prediction Division unified nonhydrostatic model. Tech. Rep. Meteor. Res. Inst., **42**, 133 pp.

Salerno, R. and A. Borroni, 2002: Hydrostatic vs. nonhydrostatic simulations in a complex orography environment. Proc. of 10th Conf. On Mountain Meteorology, 299-302, AMS.

Salerno, R., 2003: Influence of nonhydrostatic effects and time integration schemes on numerical simulations in a complex orography environment. Proc. of ICAM/MAP 2003, 230-233, MeteoSwiss Publ. No. 66.

Smolarkiewicz, P.K., L.G. Margolin, and A.A. Wyszogrodzki, 2001: A Class of Nonhydrostatic Global Model. J. Atmos. Sci., **58**, 349-364.

Tapp, M.C. and P.W. White, 1976: A Nonhydrostatic Mesoscale Model. Quart. J. Roy. Meteor. Soc., **102**, 277-296.